# REVERSE TIME MIGRATION IN TILTED TRANSVERSELY ISOTROPIC MEDIA

Linbin Zhang*

Department of Material Science and Engineering, University of California,

Berkeley, CA94720, USA

James W. Rector III

Department of Civil and Environmental Engineering, University of California,

Berkeley, CA94720, USA

G. Michael Hoversten

Earth Science Division, Lawrence Berkeley National Laboratory, Berkeley, CA94720,

USA

- email: lbzhang@lbl.gov.
- Mailing address: Linbin Zhang
  Earth division, Lawrence Berkeley National Laboratory
  One Cyclotron, MS 90-1116
  Berkeley, CA 94720

## ABSTRACT

This paper presents a reverse time migration (RTM) method for the migration of shot records in tilted transversely isotropic (TTI) media. It is based on the tilted TI acoustic wave equation that was derived from the dispersion relation. The RTM is a full depth migration allowing for velocity to vary laterally as well as vertically and has no dip limitations. The wave equation is solved by a tenth-order finite difference scheme. Using 2D numerical models, we demonstrate that ignoring the tilt angle will introduce both lateral and vertical shifts in imaging. The shifts can be larger than 0.5 wavelength in the vertical direction and 1.5 wavelength in the lateral direction.



**Keywords:** tilted transversely isotropic (TTI) media, reverse-time migration (RTM).


## INTRODUCTION

Field and theoretical studies show that many sedimentary rocks exhibit anisotropy. Ignoring anisotropy in migration may lead to large positional errors (Larner and Cohen, 1993) or a complete loss of steeply dipping structures (Martin et al., 1992). In recent years several authors have developed migration algorithms for anisotropic media. The Kirchhoff method (Ball, 1995; Kendall et al., 2001; Grech et al., 2002) is the most popular method because it is fast, especially for 3D, there is no limit on the dip angle of the reflector, and it is robust compared to finite-difference techniques. However Kirchhoff migration has difficulties in complex geological structures where multipathing

occurs. One-way wave equation methods (Ristow, 1998,1999; Le Rousseau, 1997) which image multiple arrivals properly through downward continuation of wavefields can sometimes produce more accurate images than Kirchoff methods (Uzcategui, 1995; Joncour et al., 2003). However, with one-way wave equation migration methods, approximations, such as steep-dip limit on finite difference methods or velocity simplification on mixed domain (Fourier domain) methods, have become so dominant that the artifacts caused by these approximations could overshadow the benefits of wave equation migration (Mulder; Plessix, 2003; Li, et al, 2003).

Verwest (1989) discussed finite difference migration for elliptically anisotropic media. Kitchenside (1993) developed finite difference schemes for transversely isotropic (TI) media. Ristow (1999) developed an implicit depth migration scheme for TI media based on optimizing the coefficients of finite difference equations. Uzcategui (1995) proposed an explicit finite difference scheme for VTI media with lateral and vertical variations of anisotropy. Le Rousseau (1997) extended the phase-shift-plus-interpolation method to TI media to accommodate lateral variations. An explicit finite difference scheme was extended to TTI media by Zhang et al. (2001) and Ferguson and Margrave (1998, 2002) used a symmetric non-stationary phase-shift (NSPS) to migrate TTI physical model data. Isaac et al. (1999) and Vestrum et al.( 1999, 2002) studied image in TTI media with Kirchhoff method.

A subset of wave equation migration methods is reverse time migration (RTM). RTM uses finite difference to solve the wave equation, but instead of extrapolating in depth, it

solves the full acoustic or elastic wave equation by extrapolation in time, allowing waves to propagate in all directions (Baysal et al., 1983; McMechan, 1983; Whitmore,1983; Yoon et al., 2003; Youn et al., 1999, 2001). RTM is a boundary value method and can handle the topography naturally. There is no limit on velocity, dip or wave field type, and evanescent wave are handled correctly. Dong and McMechan (1993) proposed a 3-D prestack reverse time migration of compressional waves in anisotropic media. Recently Biondi and Shan (2002) found that RTM technique is very useful for imaging both overturned reflections and prismatic reflections in more complex models.

In this paper, we develop a P-wave RTM method for tilted transversely isotropic (TTI) media, and we investigate how tilt angle can effect image quality and positioning of reflections. Our RTM algorithm uses a new P-wave acoustic wave equation for TTI media (Zhang et al., 2003).

## THE ALGORITHM

The procedure for prestack reverse-time migration for anisotropic media follows the corresponding algorithm for isotropic media. The difference is the use of an anisotropic, rather than an isotropic, wave equation for extrapolation of the data.

The anisotropic migration for a common shot dataset consists of three main steps: first, forward-propagated wavefields from the source to all grid points; second, backward-propagation of the reverse-time data records; third, application of the imaging condition.

The wavefields from the source are obtained by solving the acoustic wave equation in TTI media with a tenth-order finite difference scheme. Based on dispersion relation (by assuming shear velocity equal zero (Alkhalifah, 1998a, b)), we derived a 2D acoustic wave equation for P-wave in TTI media (Zhang et al., 2003):

$$\frac{\partial^2 P}{\partial t^2} = (V_{P_0}^2 \sin^2\phi + V^2(1+2\eta)\cos^2\phi)\frac{\partial^2 P}{\partial^2 x} + (V_{P_0}^2 \cos^2\phi + V^2(1+2\eta)\sin^2\phi)\frac{\partial^2 P}{\partial^2 z}$$
$$+ (V_{P_0}^2 - V^2(1+2\eta))\sin 2\phi \frac{\partial^2 P}{\partial x \partial z} - V_{P_0}^2 V^2 \eta(2 - 3\sin^2 2\phi)\frac{\partial^4 F}{\partial x^2 \partial z^2} - \frac{1}{2}V_{P_0}^2 V^2 \eta \sin^2 2\phi \frac{\partial^4 F}{\partial z^4}$$
$$+ V_{P_0}^2 V^2 \eta \sin 4\phi \frac{\partial^4 F}{\partial x \partial z^3} - V_{P_0}^2 V^2 \eta \sin 4\phi \frac{\partial^4 F}{\partial x^3 \partial z} - \frac{1}{2}V_{P_0}^2 V^2 \eta \sin^2 2\phi \frac{\partial^4 F}{\partial x^4} \qquad (1)$$

where:

$$P = \frac{\partial^2 F}{\partial t^2} \qquad (2)$$

$$V = V_{P_0}\sqrt{1+2\delta}\ ,\ \eta = \frac{\varepsilon - \delta}{1+2\delta}$$

V is the NMO velocity. P is pressure. δ and ε are the Thomsen anisotropic parameters ( Thomsen, 1986). $V_{P_0}$ is the vertical velocity. $\phi$ is the title angle with respect to the vertical direction and a function of position( x, z). $F$ is the wavefield. Equation (4.1) assumes a constant density. These equations are fourth-order partial differential equations in t, x and z. In this study, the $10^{th}$ order in space and second order in time finite difference method (FD) is used to solve equations (1) and (2). The FD coefficients were obtained by the

optimized method proposed by Rector et al (2002). The finite difference equations for equation (1) and (2) are:

$$\begin{aligned} P(x,z,t_{k+1}) &= 2P(x,z,t_k) - P(x,z,t_{k-1}) + A + s(t)\delta(x-x_s)\delta(z-z_s) \\ F(x,z,t_{k+1}) &= 2F(x,z,t_k) - F(x,z,t_{k-1}) + \Delta t^2 P(x,z,t_k) \end{aligned} \tag{3}$$

where A is the right hand side of equation (1) with finite difference approximation to the spatial derivatives. The source is located at $(x_s, z_s)$ with the source time function $s(t)$ .

Backward propagation of the recorded data is a boundary value problem. It starts from all receiver locations used for a single shot gather, with the recorded traces in the reverse time direction. The backward propagated wave fields are implemented by solving the equations:

$$\begin{aligned} P(x,z,t_{k-1}) &= 2P(x,z,t_k) - P(x,z,t_{k+1}) + A \\ F(x,z,t_{k-1}) &= 2F(x,z,t_k) - F(x,z,t_{k+1}) + \Delta t^2 P(x,z,t_k) \end{aligned} \tag{4}$$

At each time step during reverse time extrapolation, the imaging condition is applied by extracting the amplitudes at all grid points that satisfy the imaging condition at that time. The standard imaging condition for prestack reverse time migration is based on the crosscorrelation in time of the source wavefield (S) with the receiver wavefield (R). For multiple sources the imaging condition would be:

$$I(x,z) = \sum_s \sum_t S_s(x,z,t) R_s(x,z,t) \qquad (5)$$

where I(x,z) is the migration image value at point (x,z); $S_s$ and $R_s$ are the forward and reverse-time wavefields at point (x,z) for the s-th source. Equation (5) is a zero-lag correlation. For each shot, the source and receiver wavefield are multipled together at each grid point at each time step and the result is added to an image plane. The image plane is summed over all the time steps and sources. Common image gathers (CIGs) can be computed by (Biondi and Shan, 2002):

$$I(x,z,x_h) = \sum_s \sum_t S_s(x+\frac{x_h}{2},z,t) R_s(x-\frac{x_h}{2},z,t) \qquad (6)$$

where $x_h$ is a subsurface offset. Equation (6) has potential application to velocity analysis. If we use the correct velocity the energy calculated by equation (6) in CIGs will focus on zero-offset.

Prior to reverse time extrapolation of the recorded common-shot wavefields, some preprocessing is required. This includes muting of the first-break to avoid the associated low-wavenumbers artifact, tapering at the time and space edges of the data to reduce artifacts associated with finite recording aperture, and reversal of the time axis.

## SYNTHETIC DATA EXAMPLES

In this section, numerical examples are presented to illustrate and evaluate the prestack migration algorithm in a variety of anisotropic situations. Some previous papers have shown the effect of anisotropy on migration (Isaac, et al. 1999; Vestrum et al., 1999,2002). In our research we use numerical examples to illustrate distortion of the migrated images when data from TTI media are migrated assuming VTI or isotropy so that we can see how the tilt angle and anisotropy affects on migration.

Figure 1 shows a four-layer velocity model. The second layer is a tilted TI medium with $V_{P0}$ =2945 m/s, ε=0.24, δ=0.1 and tilt angle $\phi=30^0$. We use the tenth-order finite-differencing to generate a 16 common shot dataset. The central frequency of wavelet is 20Hz. A 500×360 regular grid with 10 m spacing in both x and z directions was used. To evaluate the quality of the migration, Figure 2 shows the zoomed depth image with our reverse time migration using the correct velocity model. We can image the structures accurately and there are no obvious artifacts. Offset-domain CIGs (Figure 3) show that the image is nicely focused at zero-offset. In contrast, the zoomed depth image and CIGs of the corresponding shot gathers obtained using VTI are shown in Figures 4 and 5. Differences observed between Figure 2 and Figure 4 are attributed only to tilt angle difference between the VTI and TTI. Neglecting the tilt angle, the interfaces beneath the anisotropic layer are moved up 64 m vertically and an imaged step is shifted about 210 m

laterally. This corresponds to 0.5 and 1.5 wavelength shifts in the vertical and horizontal directions, respectively. Figure 5 shows that the energy focused at zero-offset is not as good as that in Figure 3. Therefore the VTI migration introduces the artifacts in Figure 4. Figures 6 and 7 show the zoomed depth image and CIGs obtained by isotropic velocity model. In Figure 6, the vertical shift is 80 m and lateral shift is approximately 220 m. The energy can not be focused at zero-offset as shown in Figure 7 and the focusing in Figure 7 is worse than that in Figure 5. As a result, the migration with the isotropic model (Figure 7) has more artifacts than that obtained by the VTI model (Figure 6). In both the VTI and isotropic models, the vertical velocity is less than the true vertical velocity in TTI model. Therefore it causes the vertical shift of the imaging step under anisotropic layer. In addiction, as we used the wrong horizontal velocity for anisotropic layer, the imaged step also has a lateral shift. Figures 8 and 9 show the imaged and CIGs using the isotropic model with the correct vertical velocities. No vertical shift is observed but a lateral shift still exists. This situation may happen in real data because we may estimate Vnmo closer to the true Vnmo.

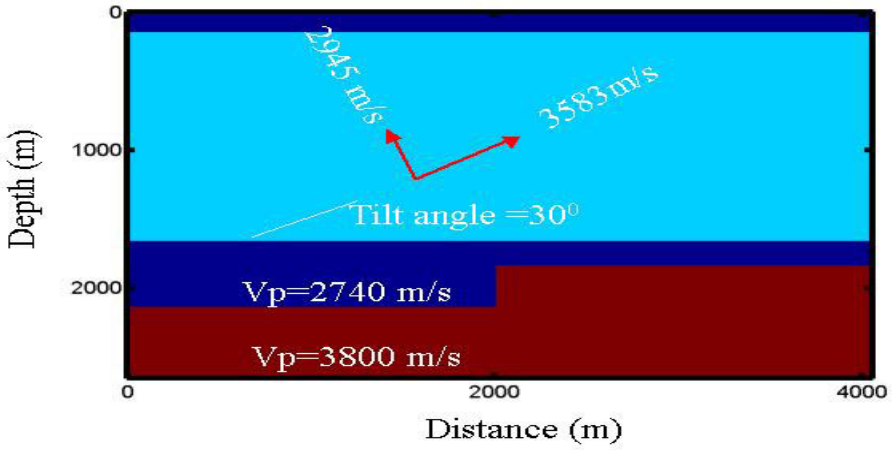


Figure 1. Velocity model. The second layer is a tilted TI medium with tilt angle $30^0$.

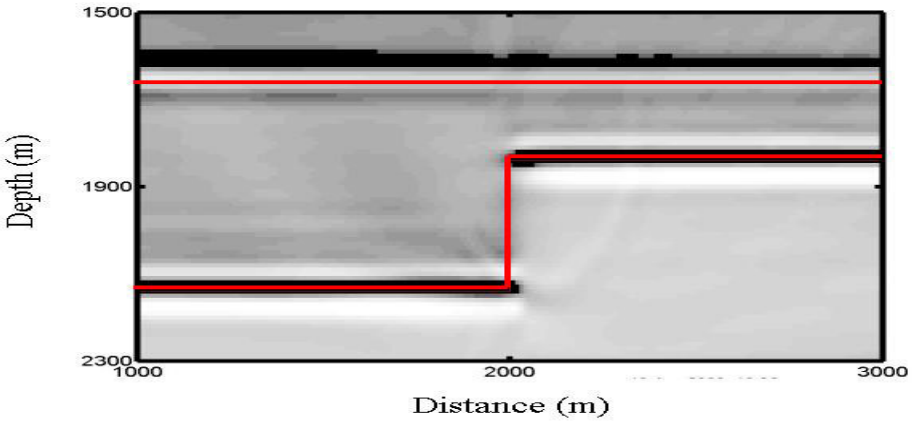


Figure 2. Reverse time migration with the TTI velocity model. The red lines are the correct boundary position.

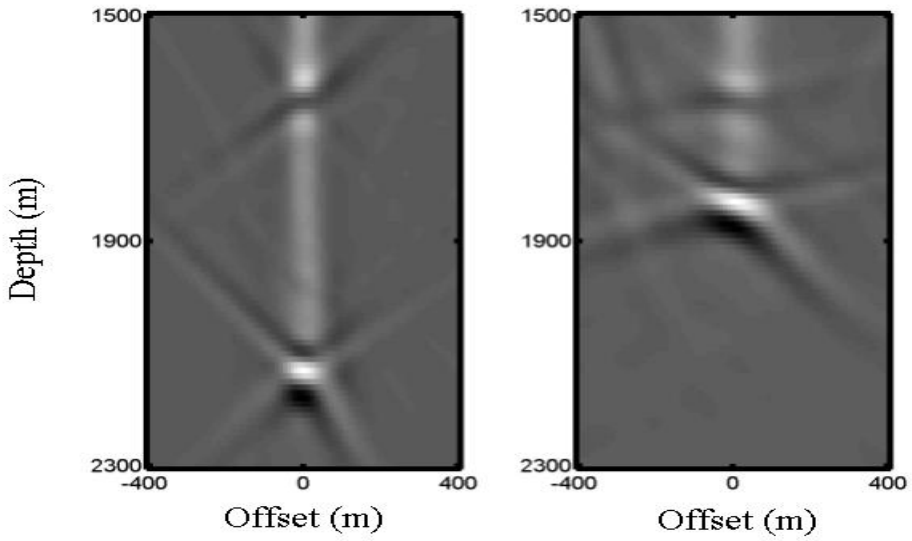


Figure 3. Offset-domain CIGs at 1500 m and 2500 m.

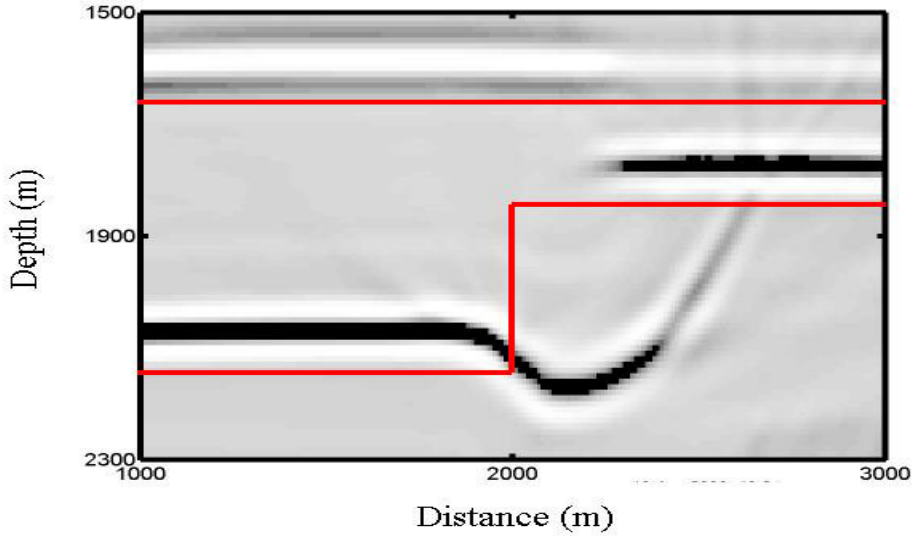


Figure 4. Reverse time migration with the VTI model. The red lines are the correct boundary position.

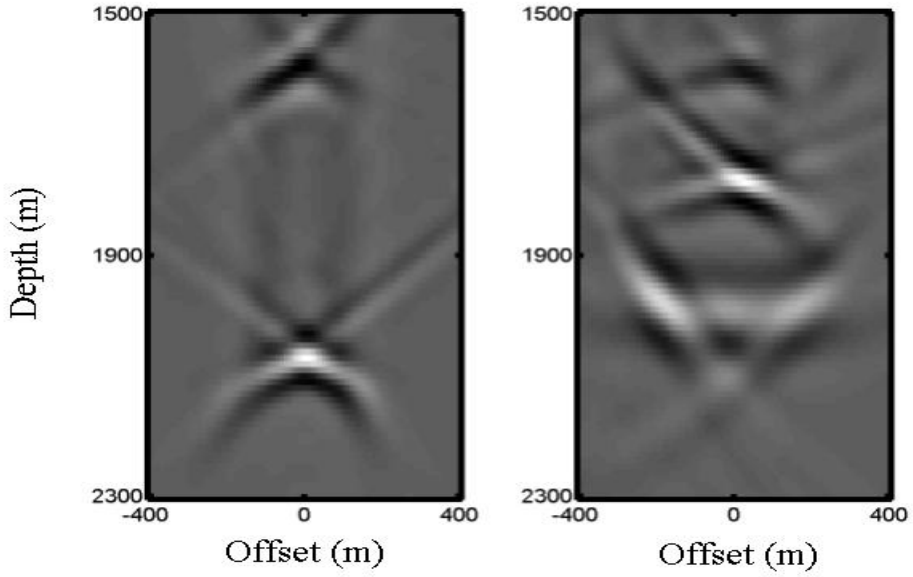


Figure 5. Offset-domain CIGs at 1500m and 2500m with the VTI model.

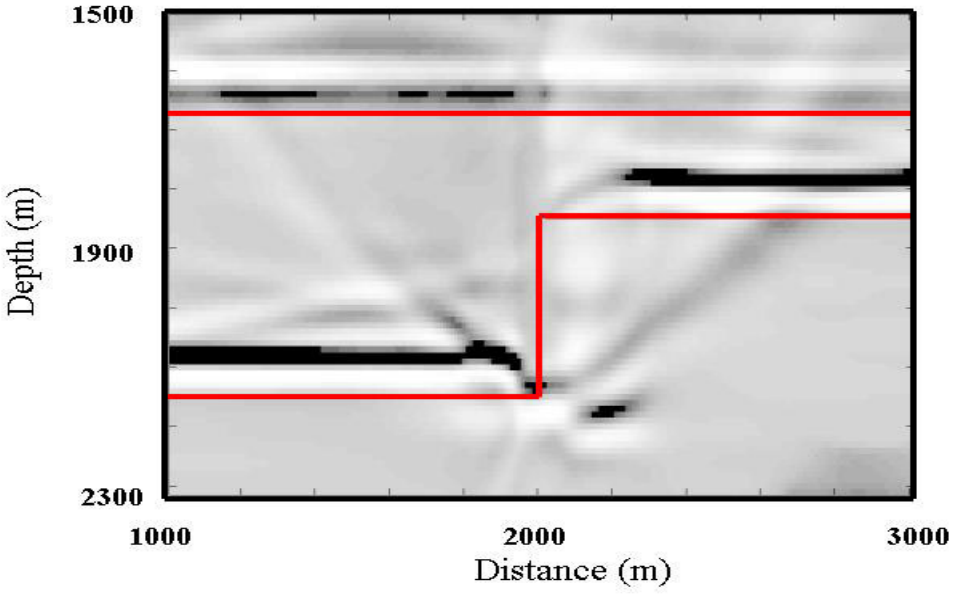


Figure 6. Reverse time migration with isotropic model. The red lines are the correct boundary position.

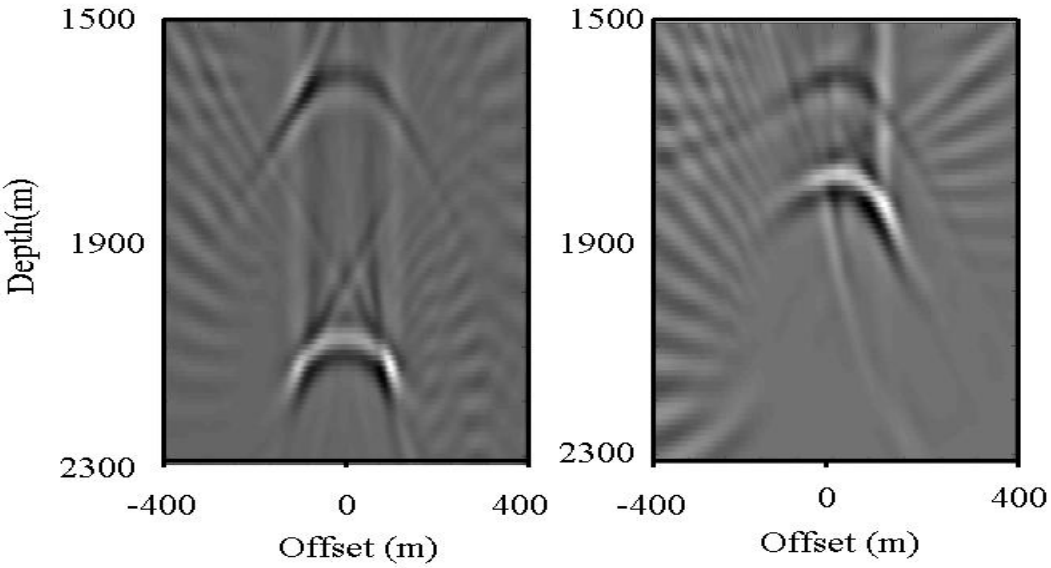


Figure 7. Offset-domain CIGs at 1500 m and 2500 m with the isotropic model.

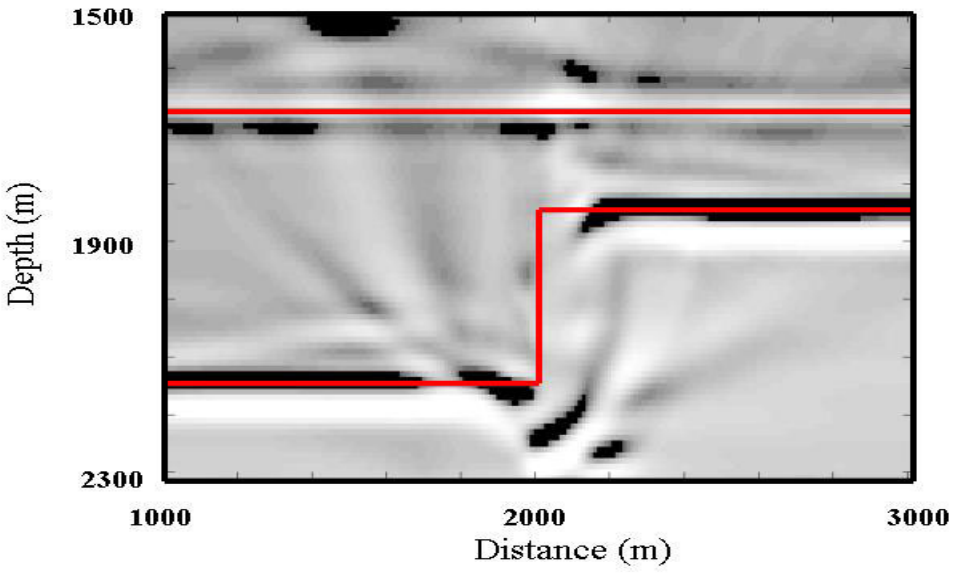


Figure 8. Reverse time migration with the correct vertical velocity in the isotropic model. The red lines are the correct boundary position.

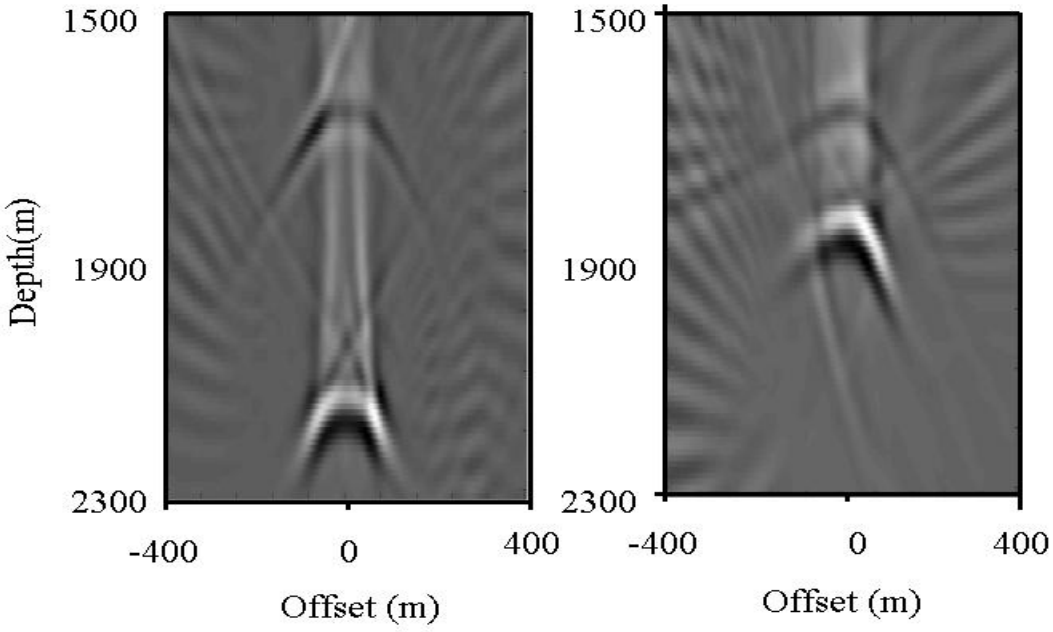


Figure 9. Offset-domain CIGs at 1500 m and 2500 m with the correct vertical velocity in the isotropic model.

To study how $\eta$ and $\phi$ effect migration, we use different $\eta$ and $\phi$ to migrate the synthetic data. Figures 10 and 11 show the lateral and vertical shifts as function of the tilt angle $\phi$ and η. The lateral and vertical shifts become larger when the errors in $\eta$ and $\phi$ become larger. The maximum lateral and vertical shifts occur when we use an isotropic model to migrate the common shot gather dataset.

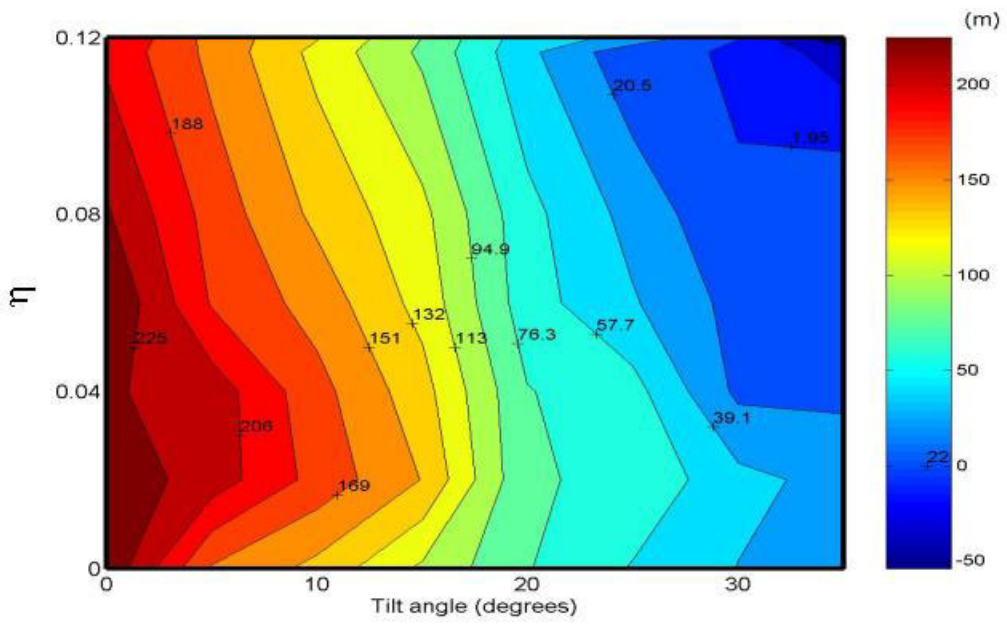


Figure 10. Lateral shifts (m) of the reflector at 1840 m as function of the tilt angle and η for the velocity model in Figure 1.

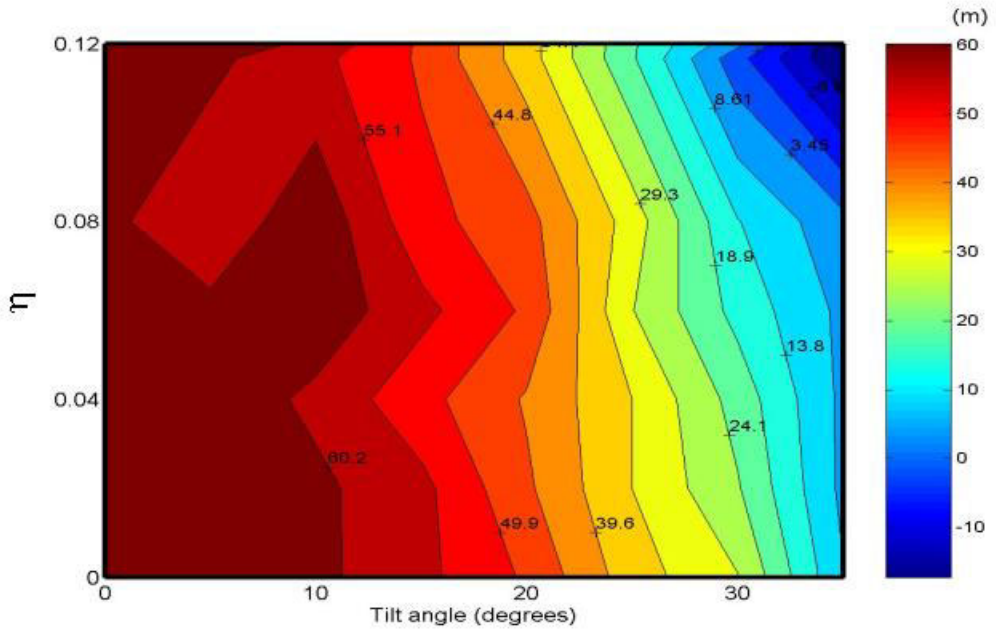


Figure 11. Vertical shifts (m) of the reflector at 1840 m as function of the tilt angle and η for the velocity model in Figure 1.

A more realistic model is shown in Figure 12. We assume that the tilt angles are normal to the lower interfaces. Synthetic 35 common shot gathers were generated by the tenth order finite-difference method with shot interval 500 m and receiver interval 25 m. The Thomsen parameters ε and δ vary from 0 to 0.25 and from 0 to 0.05, linearly from the sea bottom to the second interface. Below second interface ε=0.25 and δ=0.05. The minimum and maximum offsets are 0 m and 8000 m. Figures 13 and 14 show the images with true TTI and VTI velocity model, respectively. The true boundaries (red lines) are overlapped on the image. Figure 14 shows that the dipping boundaries can not be imaged

well. To see the mispositioning due to ignoring the tilt angle more clearly, we enlarge part of the VTI image. Figure 15 shows the vertical and horizontal mispositioning that result from ignoring the tilt angle and the anisotropy. The lateral and vertical shifts can be larger than 250 m from the true location.

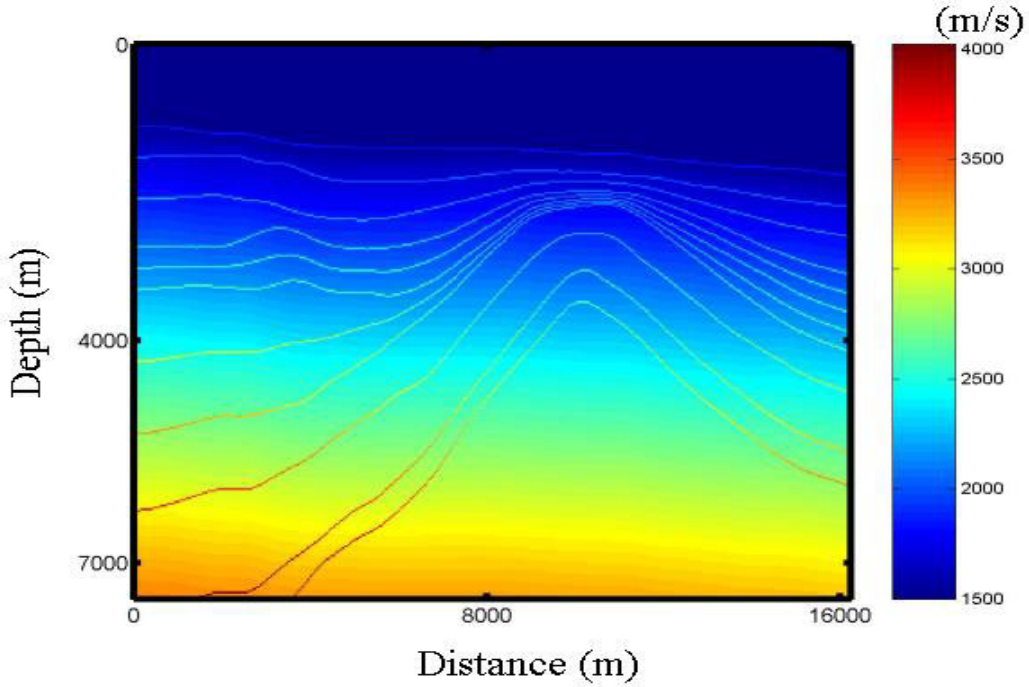


Figure 12. Vertical velocity model.

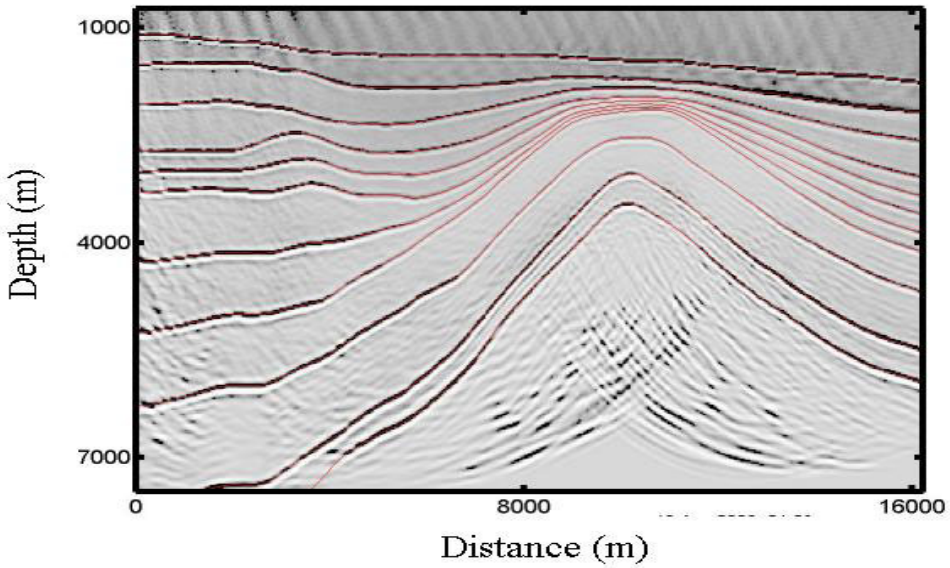

Figure 13. Imaging with the correct TTI model. The red lines are the correct boundary positions.

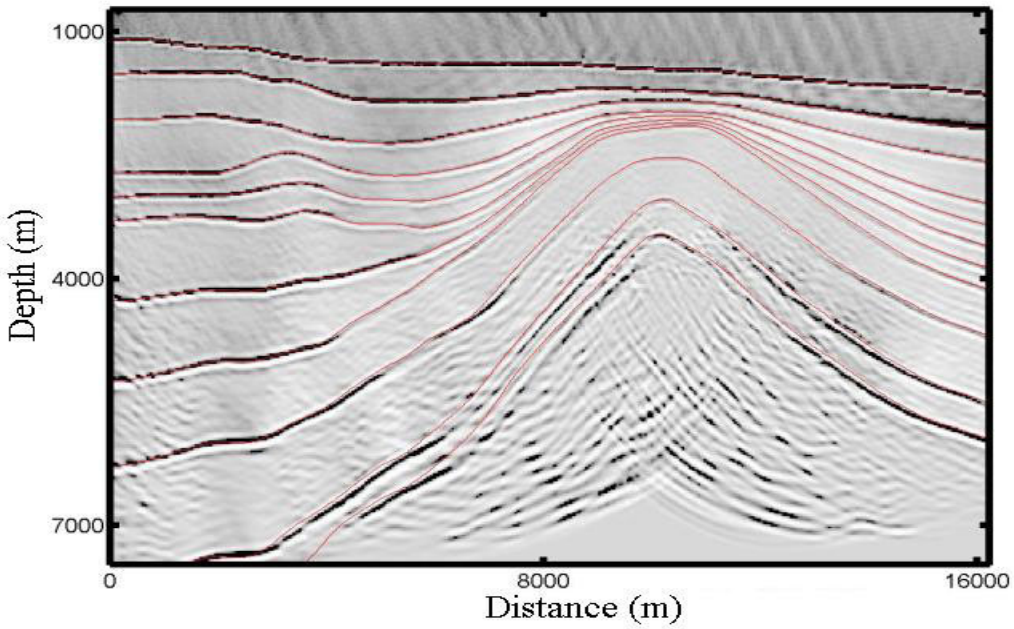


Figure 14. Imaging with the VTI model. The red lines are the correct boundary positions.

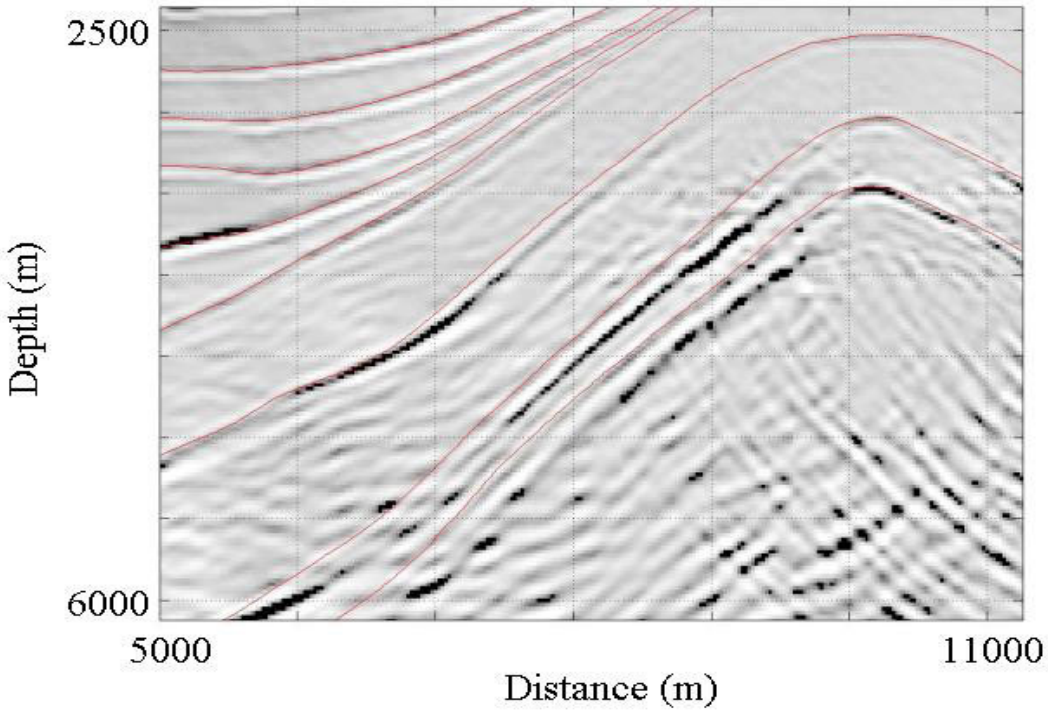


Figure 15. Imaging with the VTI model. The red lines are the correct boundary positions.

# CONCLUSIONS

It was well-known that anisotropy can cause lateral and vertical mispositioning. In this research we investigate tilt angle effects on migration by comparing VTI and TTI image. Based on the acoustic TTI wave equation, we developed a reverse time migration algorithm. The RTM method uses shot gathers as input and produces a depth image. Therefore, all intermediate processing steps such as deconvolution, multiple suppression and other signal extraction or enhancement steps used in conventional processing are not required. It also can be applied in models with strong velocity contrasts.

Numerical examples demonstrate both the vertical and the horizontal mispositioning that result from ignoring the tilt angles. These vertical and lateral shifts depend on tilt angle and $\eta$. The shifts could be much larger than 1.5 wavelength when we use VTI velocity model to migrate a TTI dataset. The positioning errors become much bigger when an isotropic velocity model is used for the TTI datasets. The mispositioning is significant because it could lead to a serious mispositioning of well locations.

The computational cost of the new method, because of the increased complexity of the wave equation, is much more than that for the corresponding isotropic migration. To process the real data in 3D a new parameter estimation technique for TTI media and a parallel version of the RTM code are needed.

## REFERENCES


Alkhalifah, T., 1998, An acoustic wave equation for anisotropic media, 68th Annual Internat. Mtg., Soc. Expl. Geophys., Expanded Abstracts, 1913-1916.

Alkhalifah, T., 1998, Acoustic approximations for processing in transversely isotropic media: Geophysics, 63,623-631.

Ball, G., 1995, Estimation of anisotropy and anisotropic 3-D prestack depth migration, offshore Zaire: Geophysics, 60, 1495-1513.

Baysal, E., Kosloff, D.,D., and Sherwood, J.W.C., 1983, Reverse time migration: Geophysics, 48, 11, 1514-1524.

Biondi, B., and Shan, G, 2002, Prestack imaging of overturned reflections by reverse time migration: 72nd Ann. Internal. Meeting, Soc. Of Expl. Geophys., Expanded Abstracts, 1284-1287.

Dong, Z., and McMechan, G.A., 1993, 3-D prestack migration of compressional waves in anisotropic media, Geophysics, 58, 79-90.

Ferguson, R.J. and Margrave, G.F., 2002, Depth imaging in anistropic media by symmetric non-stationary phase shift, Geophysical prospecting, 50, 281-288.

Ferguson, R. J. and Margrave, G. F., 1998, Depth migration in TI media by nonstationary phase shift, 68th Ann. Internat. Mtg: Soc. of Expl. Geophys., 1831-1834.

Grech, M.G., Lawton, D. C. and Gray, S. H., 2002, A multi-offset vertical seismic profiling experiment for anisotropy analysis and depth imaging: Geophysics, 67, 348-354.

Isaac, J.H. and Lawton, D.C., 1999, Image mispositioning due to dipping TI media: A physical seismic modeling study, Geophysics, 64,1230-1238.

Joncour, F., Duquet, B., Svay-Lucas, J. and Derouillat, J., 2003, Stable wavefield paraxial extrapolator for P and S waves in VTI media, 73rd Ann. Internat. Mtg.: Soc. of Expl. Geophys., 965-968.

Kendall, R.R., Gray, S. and Miao, X., 2001, Anisotropic Prestack Depth Migration for Multicomponent Data - Methodology and Examples, 63rd Mtg.: Eur. Assn. Geosci. Eng., Session: L-30.

Kitchenside,P.W., 1993, 2D anisotropic migration in space-frequency domain, Journal of seismic exploration, 2,7-22.

Larner, K. and Cohen, J. K., 1993, Migration error in transversely isotropic media with linear velocity variation in depth: Geophysics, 58, 1454-1467.

Le Rousseau, J. H., 1997, Depth migration in heterogeneous, transversely isotropic media with the phase-shift-plus-interpolation method, 67th Ann. Internat. Mtg: Soc. of Expl. Geophys., 1703-1706.

Li, Z., Su, C., Bauske, W., Tadepalli, S., Kirchhoff or wave equation? 73rd Ann. Internat. Mtg: Soc. of Expl. Geophys., 1005-1007.

Martin, D., Ehinger, A. and Rasolofosaon, P. N. J., 1992, Some aspects of seismic modeling and imaging in anisotropic media using laser ultrasonics, 62nd Ann. Internat. Mtg: Soc. of Expl. Geophys., 1373-1376.

McMechan, G. A., 1983, Migration by extrapolation of time-dependent boundary values: Geophys. Prosp., 31, 413-420.

Mulder, W., Plessix, R.,2003, One-way and two-way wave-equation migration, 73rd Ann. Internat. Mtg: Soc. of Expl. Geophys., 881-884.

Ristow, D., 1998, 3-D finite difference migration in azimuthally anisotropic media, 68th Ann. Internat. Mtg: Soc. of Expl. Geophys., 1823-1826.

Ristow, D., 1999, Migration of transversely isotropic media using implicit finite difference operator, Journal of seismic exploration, 8,39-55.

Thomsen, L., 1986, Weak elastic anisotropy, Geophysics, 51, 1954-1966.

Uzcategui, O., 1995, 2-D depth migration in transversely isotropic media using explicit operators: Geophysics, 60, 1819-1829.

VerWest, B. J., 1989, Seismic migration in elliptically anisotropic media: Geophys. Prosp., 37, 149-166.

Vestrum, R.W., Lawton, D.C. and Schmid, R., 1999, Imaging structures below dipping TI media, Geophysics, 64, 1239-1246.

Vestrum, R.W., 2002, 2D and 3D anisotropic depth migration case histories, 72nd Ann. Internat. Mtg: Soc. of Expl. Geophys., 1256-1259.

Whitmore, N.D., 1983, Iterative depth migration by backward time propagation: 53rd Ann. Internat. Mtg, Soc. of Expl. Geophys., Expanded abstracts, 827-830.

Yoon, K., Shin, C., Suh, S., Lines, L. R. and Hong, S., 2003, 3D reverse-time migration using the acoustic wave equation: An experience with the SEG/EAGE data set: The Leading Edge, 22, no. 1, 38-41.

Youn, O.K. and Zhou, H.-W., 2001, Depth imaging with multiples: Geophysics, 66, 246-255.

Youn, O. and Zhou, H. -W., 1999, Depth imaging with multiples, 69th Ann. Internat. Mtg: Soc. of Expl. Geophys., 1182-1185.

Zhang, J., Verschuur, D. J. and Wapenaar, C. P. A., 2001, Depth migration of shot records in heterogeneous, tranversely isotropic media using optimum explicit operators: Geophys. Prosp., 49, 287-299.

Zhang, L., Rector, J. and Hoversten, M., 2003, An acoustic wave equation for modeling in tilted TI media, 73rd Ann. Internat. Mtg.: Soc. of Expl. Geophys., 153-156.